

# **Reliability, Robustness and Failure Mechanisms of LED Devices**

**Yannick Deshayes and Laurent Béchou**

**ISTE  
PRESS**



**ELSEVIER**

**Durability, Robustness and Reliability of Photonic Devices  
Set**

coordinated by  
Yannick Deshayes

---

# **Reliability, Robustness and Failure Mechanisms of LED Devices**

---

*Methodology and Evaluation*

Yannick Deshayes  
Laurent Béchou

**ISTE**  
PRESS



First published 2016 in Great Britain and the United States by ISTE Press Ltd and Elsevier Ltd

Apart from any fair dealing for the purposes of research or private study, or criticism or review, as permitted under the Copyright, Designs and Patents Act 1988, this publication may only be reproduced, stored or transmitted, in any form or by any means, with the prior permission in writing of the publishers, or in the case of reprographic reproduction in accordance with the terms and licenses issued by the CLA. Enquiries concerning reproduction outside these terms should be sent to the publishers at the undermentioned address:

ISTE Press Ltd  
27-37 St George's Road  
London SW19 4EU  
UK

[www.iste.co.uk](http://www.iste.co.uk)

Elsevier Ltd  
The Boulevard, Langford Lane  
Kidlington, Oxford, OX5 1GB  
UK

[www.elsevier.com](http://www.elsevier.com)

#### Notices

Knowledge and best practice in this field are constantly changing. As new research and experience broaden our understanding, changes in research methods, professional practices, or medical treatment may become necessary.

Practitioners and researchers must always rely on their own experience and knowledge in evaluating and using any information, methods, compounds, or experiments described herein. In using such information or methods they should be mindful of their own safety and the safety of others, including parties for whom they have a professional responsibility.

To the fullest extent of the law, neither the Publisher nor the authors, contributors, or editors, assume any liability for any injury and/or damage to persons or property as a matter of products liability, negligence or otherwise, or from any use or operation of any methods, products, instructions, or ideas contained in the material herein.

For information on all our publications visit our website at <a href="http://store.elsevier.com/">http://store.elsevier.com/</a>
--

© ISTE Press Ltd 2016

The rights of Yannick Deshayes and Laurent Béchou to be identified as the authors of this work have been asserted by them in accordance with the Copyright, Designs and Patents Act 1988.

---

British Library Cataloguing-in-Publication Data

A CIP record for this book is available from the British Library

Library of Congress Cataloging in Publication Data

A catalog record for this book is available from the Library of Congress

ISBN 978-1-78548-152-9

---

# **Reliability, Robustness and Failure Mechanisms of LED Devices**



---

## Preface

---

The tremendous growth of optoelectronic technologies for information and communications technology (ICT) and public lighting, which have marked their presence in the market over the past 20 years, is mainly due to the transmission capacity through optic fiber and the performance achieved by optoelectronic components. Since the 1990s, the latter have replaced the wired telecommunication networks in copper, limited to speeds of  $100 \text{ Mbit.s}^{-1}$  on average. Since the 2000s, the emergence of devices based on GaN has allowed for the gradual replacement of traditional lighting technologies. The performance of optoelectronic technologies for ICT has already reached above  $160 \text{ GB.s}^{-1}$ , thanks to the wavelength multiplexing technology  $\lambda$ . To date, their performance has not stopped increasing and they have replaced the technology of electronic interconnections. Currently, the high bandwidth available on a single-mode optical fiber and the control of manufacturing processes of materials III-V are in competition with the technologies developed in electronics primarily based on silicon.

In the case of GaAs technology, we have now reached the order of performance of a few Watts with an average lifetime of 100,000 hours.

However, the control of manufacturing techniques of optoelectronic systems is more delicate than that of microelectronic technologies for two major reasons:

- 1) The optical function requires a precise alignment between the chip and the lens system as well as the materials whose optical properties must remain constant over time.

- 2) The manufacturing cost of optical technologies is relatively higher than that of electronic systems, especially for embedded systems. The basic structure of a light emitting diode (LED) may comprise more than 10 epitaxial layers, far exceeding the complex structure of electronic transistors.

A review of the main applications of LEDs, whose emission is in the near infrared (IR) is proposed in this book.

A state-of-the-art of the technologies of components and IR LED systems indicating the physical properties, structures as well as architecture of components is also provided.

Yannick DESHAYES

Laurent BÉCHOU

July 2016

---

# Contents

---

<b>Preface</b> . . . . .	vii
<b>Chapter 1. State-of-the-Art of Infrared Technology</b> . . . . .	1
1.1. Introduction . . . . .	1
1.2. Compound materials III-V . . . . .	2
1.2.1. Historical introduction . . . . .	2
1.2.2. Physical properties of the III-V compounds emission. . . . .	4
1.2.3. Ternary and quaternary compounds. . . . .	18
1.3. Light-emitting diodes . . . . .	21
1.3.1. Introduction . . . . .	21
1.3.2. Epitaxial structures . . . . .	22
1.3.3. LED assembly. . . . .	32
1.4. Applications . . . . .	38
1.4.1. Infrared remote control systems . . . . .	38
1.4.2. Autofocus . . . . .	40
1.4.3. Space. . . . .	42
1.5. Conclusion . . . . .	44
<b>Chapter 2. Analysis and Models of an LED</b> . . . . .	45
2.1. Introduction . . . . .	45
2.2. Physicochemical analysis . . . . .	46
2.2.1. Context and objectives . . . . .	46
2.2.2. Analysis adapted to casing. . . . .	46
2.2.3. Analysis adapted to the chip . . . . .	52
2.3. Electro-optical analysis . . . . .	56
2.3.1. Current–voltage characteristics . . . . .	57
2.3.2. Spectral characteristics . . . . .	60



2.4. Initial characterizations of 935 nm LEDs . . . . .	68
2.4.1. Technological evaluation. . . . .	68
2.4.2. Electro-optical characterization and electrical modeling of the LED . . . . .	70
2.5. Conclusion . . . . .	78
<b>Chapter 3. Physics of Failure Principles . . . . .</b>	<b>79</b>
3.1. Introduction . . . . .	79
3.2. Aging tests . . . . .	80
3.2.1. Sequence of aging campaign. . . . .	80
3.3. Failure signatures . . . . .	86
3.3.1. Functional parameters . . . . .	86
3.3.2. Electrical failure signatures . . . . .	88
3.3.3. Optical failure signatures. . . . .	93
3.4. Physics of failures . . . . .	95
3.4.1. Mechanisms related to transport phenomena . . . . .	95
3.4.2. Electron transition mechanisms . . . . .	110
3.4.3. Model of a defect in a crystal . . . . .	113
3.4.4. Impact of defects on emission properties . . . . .	114
3.5. Conclusion . . . . .	115
<b>Chapter 4. Methodologies of Reliability Analysis. . . . .</b>	<b>117</b>
4.1. Introduction . . . . .	117
4.2. Method based on the physics of failures . . . . .	118
4.2.1. Acceleration and aggravation factor. . . . .	118
4.2.2. Estimation of lifetime distribution. . . . .	121
4.2.3. Line input sorting of a component. . . . .	124
4.3. Digital methods . . . . .	127
4.3.1. General points . . . . .	127
4.3.2. Application: cases of emissive optoelectronic systems. . . . .	128
4.3.3. Conclusions . . . . .	130
4.4. A new approach . . . . .	131
4.4.1. Context and method . . . . .	131
4.4.2. LEDs studied . . . . .	131
4.4.3. Gamma irradiation . . . . .	149
4.4.4. Neutron irradiation . . . . .	153
4.5. Conclusion . . . . .	159
<b>Bibliography . . . . .</b>	<b>161</b>
<b>Index . . . . .</b>	<b>163</b>

---

# State-of-the-Art of Infrared Technology

---

## 1.1. Introduction

Optoelectronic technologies have appeared on the market in the recent years. They started by replacing the copper wired telecommunications networks. In addition, they are in competition with integrated electronic technologies, particularly at the level of interconnection. The transmission capacity through optical fiber increases a likelihood of improved performance, which cannot be foreseen in electronics. However, the field of optoelectronics techniques is still in the development stage. Furthermore, two essential problems arise:

- the manufacturing cost of optical technologies is higher than that of conventional electronic systems, especially for the treatment of data in embedded systems;
- the reliability of optoelectronic systems is difficult to understand. Their complexity (chip and assembly) makes the study and analysis of failures more difficult. It becomes imperative to consider these two essential problems to comprehend the optical alignment for the assembly and the drifts of the electro-optical parameters of the chip.

This chapter will focus on the second problem: the evaluation and identification of degraded areas on a light emitting diode (LED). The main challenge lies in the impossibility to study all the existing optoelectronic systems. Therefore, we chose infrared-emitting components as the research subject to study electroluminescent diodes.

This book introduces the III-V materials associated with infrared optoelectronic components. Furthermore, it provides an overview of the main optoelectronic applications of emission. The systems under study will be elaborated by providing a general approach to failure analysis. Meanwhile, the structure of the systems will be discussed briefly and the associated critical problems will also be highlighted.

## 1.2. Compound materials III-V

### 1.2.1. Historical introduction

The appearance of laser transmitters dates back to the 1960s. The two main developments towards miniaturization have been the mastering of the production of III-V semiconductor substrates, on the one hand, and the mastering of epitaxial techniques, on the other.

The first polycrystalline III-V ingot was manufactured in 1951, from a mixture of antimony and indium. The semiconducting properties of these materials, such as optical index, bandgap to direct gap and the possibility of achieving parallel mirrors of crystalline quality, were the starting point of the study of compounds, combining an element of the third column of the *Mendeleev* table, such as Al, Ga and In, and an element of the fifth column such as P, As and Sb.

In 1954, *Gremmelmaier* obtained the first single crystals of gallium arsenide and indium arsenide using the *Czochralski* draw, allowing it to achieve p-n photoconductive junctions.

In the 1960s, the rules governing the main III-V compounds for optoelectronic applications shown in Figure 1.1 were inferred:

- the bandgap length decreases with the atomic number of the elements constituting the crystal;
- when the crystal formed by its elements have the same lattice parameter, the III-V material presents a gap and a higher melting point than that of its constituents;
- the compounds of the lightest elements work under indirect-transition conditions;
- the compounds of the heaviest elements work under direct-transition conditions.

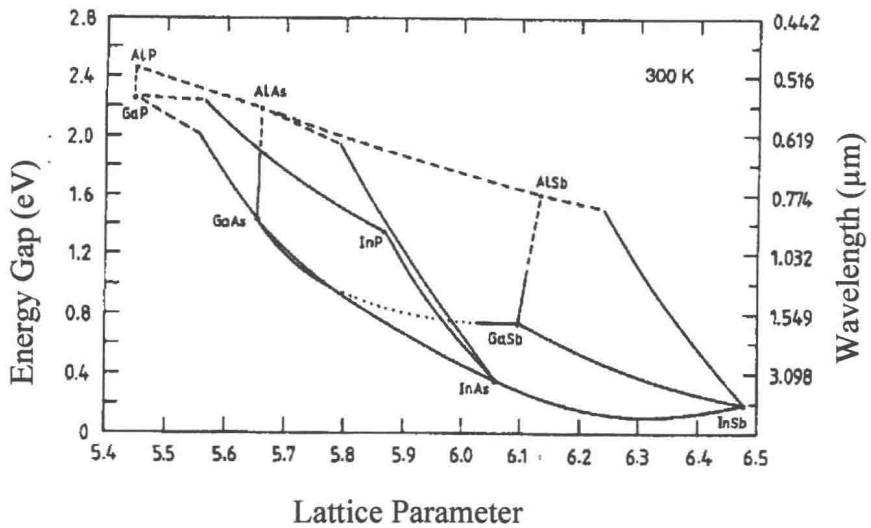


**Figure 1.1.** Schematic of different III-V compounds for optoelectronic applications with their lattice parameter

Two compound materials, GaAs and InP, have established themselves due to their specific emission characteristics:

- materials that have a gap allow the emission in the near infrared;
- lattice parameter only evolves with certain elements of substitution.

The components consist of GaAs that appears as a good candidate for optical pumping in the EDFA Erbium Doped Fibre Amplifier at 1,550 nm wavelength. Their wavelength emissions are about 980 nm that correspond to the pumping of the energy levels of erbium. The wavelengths of the components constituted on the base of InP range between 1,310 and 1,550 nm. These two wavelengths correspond to the minimum optical absorption of an optical fiber shown in Figure 1.2. Two minima are observed, located at 1,310 nm with  $0.3 \text{ dB.km}^{-1}$  and 1,550 nm with  $0.2 \text{ dB.km}^{-1}$ . The components on InP are therefore well suited for long distance emissions in an optical fiber.

The entirety of these systems has been the basis for international fiber optic communications.

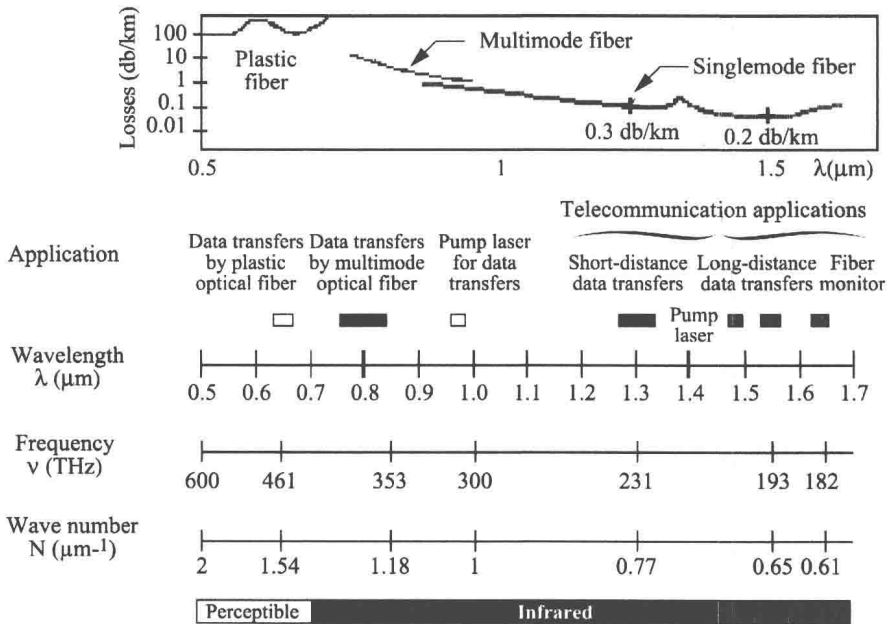


**Figure 1.2.** Schematic of mitigation in an optical fiber. For a color version of the figure, see [www.iste.co.uk/deshayes/reliability1.zip](http://www.iste.co.uk/deshayes/reliability1.zip)

**1.2.2. Physical properties of the III-V compounds emission**

The electronic states in a crystalline solid, and more particularly in a semiconductor, are divided into energy bands where they are identified by a continuously varying index: the wave vector  $\vec{k}$ . This section presents the mathematical techniques that take into account the interactions between the light and its energy states that are continuously distributed. This will allow us to describe how the interactions take place between light and covered semiconductors.

**1.2.2.1. Dipolar elements in a semiconductor direct gap**

Consider a volume semiconductor  $\Omega_r$  whose wave functions of the eigenstates  $|\Psi_{n,k}$  of energy  $E_{n,k}$  are the functions of Bloch-Foquet:

$$\Psi_{n,k}(\vec{r}) = \frac{u_{n,k}(\vec{r})}{\sqrt{\Omega_r}} \exp(i\vec{k} \cdot \vec{r}) \quad [1.1]$$

where  $u_{n,k}(\vec{r})$  represents the periodicity of the crystal. The functions  $u_{n,k}(\vec{r})$  are normalized on the volume of the elementary cell  $\Omega_i$ , which means that:

$$\int_{\Omega_i} |u_{n,k}(\vec{r})|^2 d^3r = \Omega_i$$

We have also standardized the stationary functions on an imaginary box of volume  $\Omega_r = N\Omega_i$ , such that:

$$\int_{\Omega_i} |\Psi_{n,k}(\vec{r})|^2 d^3r = 1$$

The consequence of this standardization of vectors lies in the fact that wave vectors  $\vec{k}$  are pseudo-quantified. Note that the procedure currently used for the pseudo-quantification in a crystalline solid is the Born-von Karman condition. To summarize, the spatial variations of the free portion of the wave function  $\exp(i\vec{k}\cdot\vec{r})$  are very slow compared to those of the atomic part  $u_{n,k}(\vec{r})$ . The free portion therefore represents the envelope of the Bloch functions.

The semiconductor considered is subjected to an electromagnetic wave whose Hamiltonian perturbation of interaction is given by:

$$W(\vec{r}, t) = W \cos(\vec{k}_{op} \cdot \vec{r} - \omega t) = -q\vec{E} \cdot \vec{r} \cos(\vec{k}_{op} \cdot \vec{r} - \omega t) \quad [1.2]$$

where  $\vec{r}$  is the operator position,  $\vec{k}_{op}$  is the wave vector of the light and  $\vec{E}$  is the electric field. The optical interaction Hamiltonian  $W(\vec{r}, t)$  will couple two states  $|\Psi_{n,k}\rangle$  and  $|\Psi_{n',k'}\rangle$ .

The probability rate (in  $s^{-1}$ ) for the electron in the band  $n$  with wave vector  $\vec{k}$  being energized in the band  $n'$  with wave vector  $\vec{k}'$  is provided by the following equation:

$$P_{n,k,n',k'} = \frac{\pi}{2\hbar} |\Psi_{n',k'}| W |\Psi_{n,k}|^2 \delta(\hbar\omega = E_{n',k'} - E_{n,k}) \quad [1.3]$$

The energy dependence of the Dirac function expresses the conservation of energy.

We now calculate the matrix element  $W_{n,k,n',k'}$ :

$$\langle \Psi_{n',k'} | W | \Psi_{n,k} \rangle = -\frac{qE}{\Omega_r} \iiint_{\text{network}} u_{n',k'}(\vec{r}) e^{i\vec{k}'\vec{r}} e^{-i\vec{k}_{op}\vec{r}} u_{n,k}(\vec{r}) e^{-i\vec{k}\vec{r}} \quad [1.4]$$

Equation [1.4] can be simplified by noting that the term in  $e^{i(\vec{k}' - \vec{k}_{op} - \vec{k})\vec{r}}$  differs slightly from the functions  $u$ . We can therefore split the integral as follows:

$$\begin{aligned} \langle \Psi_{n',k'} | W | \Psi_{n,k} \rangle &= -\frac{qE}{\Omega_r} \sum_i e^{i(\vec{k}' - \vec{k}_{op} - \vec{k})\vec{r}_i} \underbrace{\iiint_{\text{cell } i} u_{n',k'}^*(\vec{r}) \vec{r} u_{n,k}(\vec{r}) d\vec{r}}_I \\ I &= \iiint_{\text{cell } i} u_{n',k'}^*(\vec{R})(\vec{r}_i + \vec{R}) u_{n,k}(\vec{R}) d\vec{R}^3 \\ I &= \iiint_{\text{cell } 0} u_{n',k'}^*(\vec{R})(\vec{R}) u_{n,k}(\vec{R}) d\vec{R}^3 \end{aligned} \quad [1.5]$$

Here  $\vec{R}$  describes the elementary cell around 0. The term “integral” in  $\vec{r}_i$  is eliminated since the Bloch functions are orthonormal between them for  $\vec{k} \neq \vec{k}'$ . This integral is therefore independent of cell  $i$ , where the integral is carried out. The calculation then becomes:

$$\Psi_{n',k'} | W | \Psi_{n,k} = -\frac{qE}{\Omega_r} I \sum_i e^{i(\vec{k}' - \vec{k}_{op} - \vec{k})\vec{r}_i} = -\frac{qE}{\Omega_r} IN \delta(\vec{k}' - \vec{k}_{op} - \vec{k}) \quad [1.6]$$

The term in point in the Kronecker function expresses the conservation of moments in the interaction between electrons and photons:  $\vec{k}' = \vec{k}_{op} + \vec{k}$ . The transitions are therefore vertical.  $u_{c,k}$  is noted as the periodic part of the Bloch function in the conduction band and  $u_{v,k}$  as the periodic part of the Bloch function in the valence band. Equation [1.6] can therefore be written as:

$$\begin{aligned} W_{vc} &= -qE r_{vc} \delta(\vec{k}' - \vec{k}_{op} - \vec{k}) \\ r_{vc} &= \frac{1}{\Omega_i} \iiint_{\text{cell } i} u_{c,k}^*(\vec{R})(\vec{R}) u_{v,k}(\vec{R}) d\vec{R}^3 \end{aligned} \quad [1.7]$$

We can connect the equation linking the matrix elements of the optical Hamiltonian interactions  $A.p$  and  $D.E$ :

$$r_{vc} = -\frac{i}{m_0 \omega_k} \rho_{vc} \quad [1.8]$$

where  $m_0$  is the mass of the electron in the vacuum and  $\hbar\omega_k$  is the energy separating the two states  $k$  of the valence and conduction band. The matrix elements are easily obtained from Kane settings. This formula is very useful because  $\rho$  is almost constant in all III-V semiconductors. Using the theory of Kane, we can show, on the first order in  $k$ , that the matrix elements are constant. We use the element under its homogeneous form  $\rho^2$  to a Kane energy  $E_p$  that leads to the following equation:

$$|r_{vc}| = \frac{\hbar}{E_g} \sqrt{\frac{E_p}{m_0}} \quad [1.9]$$

Another term is introduced,  $\chi_{vc}$ . The simple calculation of this item is done by introducing the principle that only the bands of heavy and light holes are active in the radiative recombination. The transitions with the spin-orbital band are neglected. The analysis reveals that this corresponds to 2/3 of the oscillator strength (characteristic of electrons bound to the matrix):

$$\chi_{vc} = \frac{2}{3} r_{vc}^2 = \frac{\hbar^2}{3E_g^2} \frac{E_p}{m_0} \quad [1.10]$$

For small gap materials, the dipolar matrix element becomes very large in comparison to the interatomic distance. This means that the electronic wave function is increasingly shifting as the gap decreases. It is known that small gap materials have a quantum behavior.

#### 1.2.2.2. Optical susceptibility of a semiconductor

We can now calculate the optical susceptibility associated with the transitions between the valence band and the conduction band. In addition to the previous assumptions, we assume that the semiconductor admits parabolic bands that are well described by their effective masses  $m_v$  and  $m_c$ . Optical transitions are vertical; here we are interested in optical susceptibility  $\chi_k(\omega)$  due to the transition towards the elements of the conduction band of the same  $k$ . Equations  $\hbar\omega = E_{n',k} - E_{n,k}$  and  $\vec{k}' = \vec{k}_{op} + \vec{k}$  indicate the relationship between energies of the conduction band  $E_c(k)$  and that of valence  $E_v(k)$  coupled by optical transition:

$$E_c(k) - E_v(k) = \frac{\hbar^2 k^2}{2} \left( \frac{1}{m_c} + \frac{1}{m_v} \right) + E_g \quad [1.11]$$



We introduce the reduced effective mass  $m_r$  to simplify the expression:

$$\frac{1}{m_r} = \frac{1}{m_c} + \frac{1}{m_v} \quad [1.12]$$

Optical susceptibility (without dimension) associated with the transition between quasi-discrete levels  $E_v(k)$  and  $E_c(k)$  is provided by:

$$\chi_k(\omega) = \frac{q^2 \chi_{vc}^2(k) T_2}{\epsilon_0 \hbar} \frac{[\omega - \omega_{vc}(k)] T_2 - i}{[\omega - \omega_{vc}(k)]^2 T_2^2 + 1} [N_c(k) - N_v(k)] \quad [1.13]$$

Here  $\chi_{vc}(k) = \chi_{vc}$  as the elements of independent matrix of  $k$  are assumed.  $\chi_{vc}(k)$  is arbitrarily oriented in a direction  $Ox$  to alleviate the notation.  $\omega_{vc} = (E_c(k) - E_v(k)) / \hbar$  and  $T_2$  is the relaxation time of electrons in the bands.  $N_c(k)$  and  $N_v(k)$  represent the density of particles (in  $\text{cm}^{-3}$ ) at  $E_v(k)$  and  $E_c(k)$  levels. The total optical susceptibility is therefore provided by the sum of [1.14] on the total values of  $k$ :

$$\chi(\omega) = 2 \sum_k \frac{q^2 \chi_{vc}^2(k) T_2}{\epsilon_0 \hbar} \frac{[\omega - \omega_{vc}(k)] T_2 - i}{[\omega - \omega_{vc}(k)]^2 T_2^2 + 1} [N_c(k) - N_v(k)] \quad [1.14]$$

The factor 2 stems from the fact that electrons have two spins by wave vector. As the dimension of the crystal is very large compared to the lattice parameter, we can consider that the wave vector forms a quasi-continuum. In this case, the sum can be transformed in an integral according to the law [1.15]:

$$2 \sum_{k \in \text{BZ}} \leftrightarrow \int_k \rho(k) d^3k \leftrightarrow \int_E \rho(E) dE \quad [1.15]$$

where  $\rho(k)$  is the density expressed in  $\text{cm}^{-3}$  and  $\rho(E)$  is the density expressed in  $1/J$ . Both densities should take into account the spin degeneracy. However, in an isotropic medium, the microscopic densities  $N_c(k)$  and  $N_v(k)$  are given by  $\rho_c(k) d^3k$  and  $\rho_v(k) d^3k$ , where we obtain the following equation:  $\rho_c(k) = \rho_v(k) = 2V / (2\pi)^3 = V / 4\pi^3$ .